Luminescent and Redox-Active Iridium(III)-Cyclometalated Compounds with Terdentate Ligands

Antonino Mamo,*,† Ivan Stefio,† Melchiorre F. Parisi,‡ Alberto Credi,§ Margherita Venturi,§ Cinzia Di Pietro,|| and Sebastiano Campagna*,||

Istituto Chimico, Facoltà di Ingegneria, Università di Catania, I-95125 Catania, Italy, Dipartimento di Chimica Organica e Biologica, Università di Messina, I-98166 Messina, Italy, Dipartimento di Chimica "G. Ciamician", Università di Bologna, I-40126 Bologna, Italy, and Dipartimento di Chimica Inorganica, Chimica Analitica e Chimica Fisica, Università di Messina, I-98166 Messina, Italy

Received June 26, 1997[⊗]

Two novel bis-terdentate Ir(III)-cyclometalated complexes, $[Ir(L1)(L1^-)]^{2+}$ (**1**) and $[Ir(L1^-)_2]^+$ (**2**), have been prepared (L1 is 2,6-bis(7′-methyl-4′-phenyl-2′-quinolyl)pyridine; $L1^-$ is its mono-anion, see Figure 1). To the best of our knowledge, **1** and **2** are the first luminescent and redox-active Ir(III)-cyclometalated bis-terdentate compounds. In acetonitrile solution, on oxidation, **2** undergoes a reversible, metal-centered, one-electron oxidation at +1.40 V, whereas **1** does not exhibit any oxidation process up to +2.00 V. On reduction, both compounds undergo four reversible ligand-centered one-electron processes. The absorption spectra of the compounds are dominated by moderately intense (ϵ in the 10^3-10^4 M^{-1} cm^{-1} range) spin-allowed metal-to-ligand charge-transfer (MLCT) bands at wavelengths longer than 350 nm and by intense (ϵ in the 10^4-10^5 M^{-1} cm^{-1} range) ligand-centered (LC) bands at shorter wavelengths. The complexes exhibit an intense luminescence both at 77 K in MeOH/EtOH, 4:1 (v/v), rigid matrix (**1**, $\lambda_{max} = 592$ nm, $\tau = 20$ μs; **2**, $\lambda_{max} = 598$ nm, $\tau = 9$ μs) and at room temperature in deoxygenated acetonitrile solution (**1**, $\lambda_{max} = 620$ nm, $\tau = 325$ ns, $\Phi = 0.005$; **2**, $\lambda_{max} = 630$ nm, $\tau = 2.3$ μs, $\Phi = 0.066$). In all cases, the emission is assigned to triplet MLCT levels (namely, Ir → L1 and Ir → $L1^-$ in **1** and **2**, respectively).

Introduction

Luminescent and redox-active polypyridine-type metal complexes are playing a key role as molecular components (building blocks) in the development of supramolecular species capable of harvesting solar energy and elaborating light information at the molecular level.[1] Most of such supramolecular species are based on ruthenium(II) and osmium(II) tris-bidentate and/or bis-terdentate building blocks.[1d,2] Recently iridium(III) species, which are known[3] to be quite interesting systems from the photochemical and redox viewpoint, have been integrated into luminescent supramolecular arrays.[4] Their use, however, is limited because almost all the luminescent and redox-active iridium(III) complexes developed so far are made up of *bidentate* polypyridine (or cyclometalating) ligands.[5] This is an unfavorable situation because terdentate polypyridine-type ligands are particularly interesting as far as the control of the geometry of supramolecular structures is concerned.[2] As a consequence, iridium(III)-based chromophores remain at the margin of this research field.

Here we report the synthesis, characterization, absorption spectra, photophysical properties, and redox behavior of the *first (to the best of our knowledge) luminescent and redox-active Ir(III)-cyclometalated bis-terdentate compounds*, **1** and **2** (Figure 1), with polypyridine-type ligands. These compounds represent the first examples of a new class of luminescent and redox-active metal complexes. It can be envisaged that, after suitable functionalization of the ligands (e.g., by derivatization of position 4), these new chromophores could be inserted into metal-based supramolecular arrays for light energy conversion, thus opening a way to supramolecular architectures containing novel useful building blocks.

Results and Discussion

Synthesis. The ligand used for the synthesis of **1** and **2** is 2,6-bis(7′-methyl-4′-phenyl-2′-quinolyl)pyridine (bmpqpy, L1;

† Università di Catania.
‡ Dipartimento di Chimica Organica e Biologica, Università di Messina.
§ Università di Bologna.
|| Dipartimento di Chimica Inorganica, Chimica Analitica e Chimica Fisica, Università di Messina.
⊗ Abstract published in *Advance ACS Abstracts,* November 1, 1997.

(1) (a) Balzani, V.; Scandola, F. *Supramolecular Photochemistry*; Ellis Horwood: Chichester, U.K., 1991. (b) Balzani, V.; Credi, A.; Scandola, F. In *Transition Metals in Supramolecular Chemistry*; Fabbrizzi, L., Poggi, A., Eds.; Kluwer: Dordrecht, The Netherlands, 1994; p 1. (c) Lehn; J.-M. *Supramolecular Chemistry—Concepts and Perspectives*; VCH: Weinheim, Germany, 1995. (d) Bignozzi, C. A.; Schoonover, J. R.; Scandola, F. *Prog. Inorg. Chem.* **1997**, *44*, 1.

(2) (a) Hammarström, L.; Barigelletti, F.; Flamigni, L.; Armaroli, N.; Sour, A.; Collin, J.-P.; Sauvage, J.-P. *J. Am. Chem. Soc.* **1996**, *118*, 11972 and references therein. (b) Harriman, A.; Ziessel, R. *Chem. Commun.* **1996**, 1707. (c) Shaw, J. R.; Sadler, G. S.; Wacholtz, W. F.; Ryu, C. K.; Schmehl, R. H. *New J. Chem.* **1996**, *20*, 749. (d) Balzani, V.; Juris, A.; Venturi, M.; Campagna, S.; Serroni, S. *Chem. Rev.* **1996**, *96*, 759 and references therein.

(3) (a) Ohsawa, Y.; Sprouse, S.; King, K. A.; De Armond, M. K.; Hanck, K. W.; Watts, R. J. *J. Phys. Chem.* **1987**, *91*, 1047. (b) Didier, P.; Ortmans, L.; Kirsch-DeMesmaeker, A.; Watts, R. J. *Inorg. Chem.* **1993**, *32*, 5239. (c) Schmid, B.; Garces, F. O.; Watts, R. J. *Inorg. Chem.* **1994**, *33*, 9. (d) Maestri, M.; Balzani, V.; Deuschel-Cornioley, C.; von Zelewsky, A. *Adv. Photochem.* **1992**, *17*, 1 and references therein.

(4) (a) van Diemen, J. H.; Hage, R.; Lempers, H. E. B.; Reedijk, J.; Vos, J. G.; De Cola, L.; Barigelletti, F.; Balzani, V. *Inorg. Chem.* **1992**, *31*, 3518. (b) Molnar, S. M.; Nallas, G.; Bridgewater, J. S.; Brewer, K. J. *J. Am. Chem. Soc.* **1994**, *116*, 5206. (c) Serroni, S.; Campagna, S.; Denti, G.; Juris, A.; Venturi, M.; Balzani, V. *J. Am. Chem. Soc.* **1994**, *116*, 9086.

(5) To the best of our knowledge, there are only two papers dealing with luminescent iridium(III) complexes containing polypyridine terdentate ligands.[6] In both cases, however, noncyclometalated compounds are reported.

(6) (a) Ayala, N. P.; Flynn, C. M., Jr.; Sacksteder, L. A.; Demas, J. N.; De Graff, B. A. *J. Am. Chem. Soc.* **1990**, *112*, 3837. (b) Vogler, L. M.; Scott, B.; Brewer, K. J. *Inorg. Chem.* **1993**, *32*, 898.

S0020-1669(97)00791-X CCC: $14.00

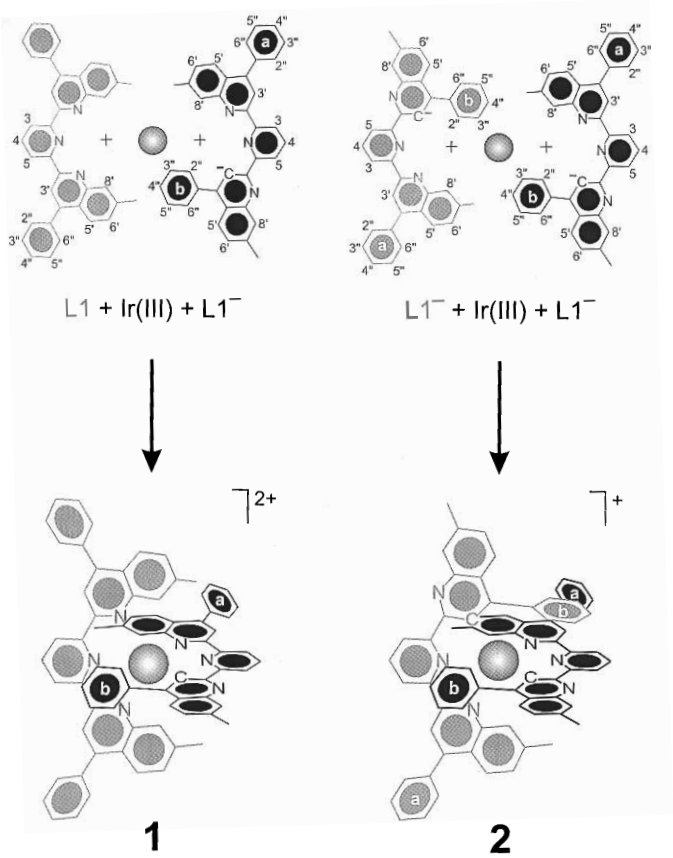

Figure 1. Schematic representation of **1** and **2**. The spheres represent the iridium(III) atoms. Shadings do not designate specific ligands but are only used for clarity purposes. For the same reason, the arrangement adopted by each ligand for complexation is shown. The phenyl substituents of $L1^-$ have been labeled *a* and *b* for convenience. According to this scheme, the phenyls of L1 in **1** are *a*-type substituents.

see Figure 1).[7] Such a ligand, in principle, can act as a terdentate ligand to chelate a metal by employing either (i) the three nitrogen atoms or (ii) two nitrogens and a C atom, giving rise to cyclometalation (bmpqpy$^-$, $L1^-$; Figure 1). It is known[3] that Ir^{III} prefers cyclometalation, so that the coordination mode (ii) was expected. The method used for the synthesis of **1** and **2** is similar to that previously employed for the synthesis[7] of $[Ru(bmqpy)_2]^{2+}$ (**3**) and $[Os(bmqpy)_2]^{2+}$. Reaction of $IrCl_3$ with bmpqpy (2 equiv) in glycerol at reflux for 24 h afforded two compounds, which after chromatographic separation were characterized (MS-FAB, mono- and bidimensional ^1H NMR) as $[Ir(bmpqpy)(bmpqpy^-)](PF_6)_2$ (**1**) and $[Ir(bmpqpy^-)_2](PF_6)$ (**2**) (for details, see Experimental Section).

NMR Characterization. The ^1H NMR data reported in Table 1 show that the resonances of the protons of the two pyridine moieties (H(3)−H(5)) and those of the two phenyl labeled *b* in Figure 1 (H(2″)−H(6″)) are shifted upfield ($\Delta\delta$ 0.08−1.38 ppm) in **2** compared to the free ligand L1. This suggests that the *b* phenyl of each of the two $L1^-$ ligands is oriented face-to-face with the pyridine moiety of the other $L1^-$ ligand, thus creating a stacking effect (Figure 1). The upfield shifts can be explained in terms of mutual diamagnetic shielding of each of these aromatic rings by the one facing it. Furthermore, the five distinct resonances observed for the two phenyl rings are the direct consequence of restricted rotation around the C(4′)−C(1″) bond and different chemical enviroments due to the asymmetric nature of the opposite $L1^-$ orthogonal ligand. The two *a* phenyls (Figure 1) are pointing out and are free to rotate around the C(4′)−C(1″) bond, thus giving rise to a multiplet (δ = 7.53 ppm, 10H).

As far as **1** is concerned, the ^1H NMR spectrum shows resonances due to both L1 and $L1^-$ ligands. With respect to the free ligand L1, the resonances of the protons of both pyridine moieties are affected by the presence of the opposite orthogonal ligand: the resonances for H(3)−H(5) of $L1^-$ move downfield ($\Delta\delta$ 0.38−0.80 ppm) because of the deshielding effect (similar to the one observed for **3**[7b]) due to the two quinoline moieties of the opposite orthogonal ligand L1, while the resonances for H(3) and H(5) of L1 move upfield ($\Delta\delta$ = 0.21 ppm), due to the shielding effect, as discussed for **2**, of the *b* phenyl of the orthogonal $L1^-$ ligand (Figure 1). Unlike the signals of H(3) and H(5), the resonance of H(4) of L1 in **1** moves downfield ($\Delta\delta$ = 0.41 ppm). The phenyl resonances further confirm the proposed structure of **1**, since the three similar phenyl groups (*a*-type; only one of them is evidenced in Figure 1) give rise to a multiplet at δ = 7.58 ppm (15 protons), while the fourth phenyl (*b*-type), involved in stacking, exhibits three distinct resonances with a marked upfield shift ($\Delta\delta$ 0.21−1.31 ppm) compared to the free ligand L1. For $L1^-$, the resonances of H(2″) and H(3″) are indistinguishable in **1** from those of H(6″) and H(5″), respectively, because they experience similar chemical environments due to the symmetry of the opposite orthogonal L1 ligand.

Redox Behavior. For the sake of simplicity, we start the discussion of the redox behavior with **2**. The oxidation pattern of this compound (Table 2, Figure 2) shows a reversible one-electron process at +1.40 V *vs* SCE which can be safely attributed to the metal-centered oxidation.[3,4] As far as reduction is concerned, four reversible one-electron processes at −1.11, −1.36, −2.01, and −2.13 V *vs* SCE are observed. The attribution of these processes is simplified on considering that **2** is composed of two identical cyclometalating ligands (Figure 1). The first two reduction processes can therefore be safely assigned to the first one-electron reduction of each ligand, and the third and fourth processes, to their second one-electron reduction. The large separation between the second and third processes (650 mV), which is correlated to the pairing energy of two electrons in the LUMO of $L1^-$, can be accounted for by considering that this orbital is mainly localized on a restricted part of the ligand, namely the noncyclometalating quinoline moiety.

On passing to **1**, it is expected that metal-based oxidation is shifted toward more positive potentials, because of the presence of the noncyclometalating ligand L1. Indeed, no oxidation process is observed for this complex up to +2.00 V *vs* SCE (Table 2, Figure 2). As for **2**, four reversible one-electron reduction processes at −0.67, −1.04, −1.37, and −1.91 V are observed. In this case, for attributing the reduction processes to specific sites, it should be considered that two different ligands are present (Figure 1). The first reduction process of **1** is assigned to the first reduction of the noncyclometalating ligand. On assuming that the pairing energy of L1 is the same as that found for an almost identical ligand in complex **3** (375 mV)[8] and considering that the separation between the first and second reductions in **1** is 370 mV (see above), we assign the second process of **1** to the second reduction of its noncyclometalating ligand. The third and fourth processes are therefore assigned to the first and second reductions of the cyclometalating ligand. This is supported by the fact that the separation between

(7) (a) Mamo, A.; Juris, A.; Calogero, G.; Campagna, S. *Chem. Commun.* **1996**, 1225. (b) Mamo, A.; Stefio, I.; Poggi, A.; Tringali, C.; Di Pietro, C.; Campagna, S. *New J. Chem.*, in press.

(8) Campagna, S.; Mamo, A.; Stille, J. K. *J. Chem. Soc., Dalton Trans.* **1991**, 2545.

Table 1. Selected Proton Chemical Shift Data[a] for the Complexes and the Free Ligand[b]

	bmpqpy$^-$ (L1$^-$)									bmpqpy (L1)			
	H_3	H_4	H_5	Ph[c]	$H_{2''}$[d]	$H_{3''}$[d]	$H_{4''}$[d]	$H_{5''}$[d]	$H_{6''}$[d]	$H_{3/5}$	H_4	$H_{3'}$	Ph
L1										8.76	8.09	8.63	7.56
1	8.16	8.01	8.42	7.53	6.18	7.03	7.21	7.03	6.27				
$\Delta\delta$	**−0.60**	**−0.08**	**−0.34**	**−0.03**	**−1.38**	**−0.53**	**−0.35**	**−0.53**	**−1.29**				
2	9.14	8.89	9.24	7.58	6.25	7.10	7.35	7.10	6.25	8.55	8.50	8.14	7.58
$\Delta\delta$	**0.38**	**0.80**	**0.48**	**0.02**	**−1.31**	**−0.46**	**−0.21**	**−0.46**	**−1.31**	**−0.21**	**0.41**	**−0.49**	**−0.02**
3[e]										9.17	8.90	8.24	7.48
$\Delta\delta$										**0.41**	**0.80**	**−0.39**	**−0.08**

[a] Chemical shifts in ppm downfield from Me_4Si. Spectra of the ligand and complexes were obtained in deuterated 1,1,2,2-tetrachloroethane (TCE). [b] Numbering pattern shown in Figure 1. [c] Resonance corresponding to phenyl ring *a*. [d] Italic protons correspond to phenyl ring *b*. [e] Used as a reference model.[7b]

Table 2. Absorption Data, Luminescence Properties, and Redox Properties of the Novel Complexes **1** and **2**[a]

		absorption	luminescence[b]					electrochemistry: $E_{1/2}$, V vs SCE	
no.	complex	λ_{max}, nm (ϵ, $M^{-1}\,cm^{-1}$)	λ_{max}, nm	τ, μs	Φ	λ_{max}, nm[c]	τ, μs[c]	oxidn	redn
1	$[Ir(L1)(L1^-)]^{2+}$	390 (44 250) 305 (52 900) 262 (73 800)	620	0.325	0.005	592	20	*d*	−0.67; −1.04; −1.37; −1.91
2	$[Ir(L1^-)_2]^+$	418 sh (6500) 357 (18 700) 313 (32 500) 238 (47 600)	630	2.3	0.066	598	9	+1.40	−1.11; −1.36; −2.01; −2.13

[a] In deoxygenated acetonitrile at room temperature unless otherwise stated. [b] Luminescence maxima are corrected for photomultiplier response. [c] In MeOH/EtOH, 4:1 (v/v), rigid matrix at 77 K. [d] No oxidation process was observed up to +2.00 V.

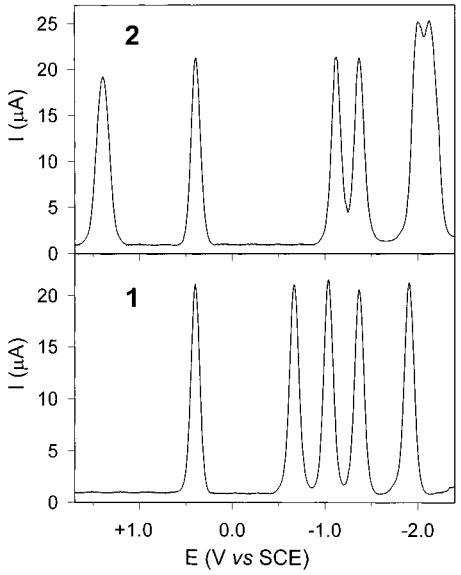

Figure 2. Differential pulse voltammograms (peak height, 75 mV; scan rate, 20 mV/s; pulse width, 40 ms) of **1** (bottom) and **2** (top) in argon-purged acetonitrile solution. Concentration of the compounds: 5×10^{-4} M. Working electrode: glassy carbon. The ferrocene peak at +0.40 V, used as a reference, is normalized by taking into account the differences in the diffusion coefficients.

the third and fourth reduction potentials of **1** (540 mV) is comparable with the pairing energy of L1$^-$ in **2** (see above).[9]

Absorption Spectra and Luminescence Properties. The absorption spectrum of **1** (Table 2, Figure 3) is dominated by an intense band peaking at 390 nm, attributed to a spin-allowed metal-to-ligand charge transfer (MLCT) transition involving L1, and by higher intensity bands, most likely ligand centered (LC)

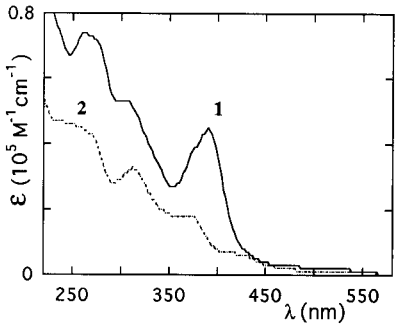

Figure 3. Absorption spectra of **1** and **2** in acetonitrile.

in nature, at shorter wavelengths. The absorption spectrum of **2** (Table 2, Figure 3) is somewhat similar in shape to that of **1** in the UV region, with the noticeable exception that it is lower in intensity. Furthermore, with respect to **1**, the MLCT band at lower energy becomes broader and a new MLCT band appears as a shoulder at 418 nm. The differences between the absorption spectra of **1** and **2** can be explained by taking into account that MLCT and LC bands involving cyclometalated ligands (which are the only possible MLCT and LC bands in **2**) are usually less intense than MLCT and LC bands involving polypyridine-type (in this case, polyquinoline) ligands;[3d] moreover, the acceptor ligands of the MLCT transition in **1** and **2** are different and the intensities of the various vibrational components of MLCT bands could be different.

The novel complexes exhibit an intense luminescence both at 77 K in MeOH/EtOH, 4:1 (v/v), rigid matrix and at room temperature in deoxygenated acetonitrile solution (Table 2; see Figure 4 for **2**). The emission is assigned to ^{3}MLCT levels in all cases (namely, Ir → L1 and Ir → L1$^-$ in **1** and **2**, respectively), on the basis of emission spectral shapes, energies, and lifetimes.[10] The similar energies of the luminescent excited states in both the complexes are justified by the fact that the less positive metal-based oxidation potential in **2** (+1.40 V)

(9) Alternatively, the second reduction process of **1** could be assigned to the first reduction of the cyclometalating ligand L$^-$; in this case, the third and fourth reduction processes should involve different ligands. This is in contrast with the large separation (540 mV) found between the latter reduction processes.

(10) Crosby, G. A. *Acc. Chem. Res.* **1975**, *8*, 231.

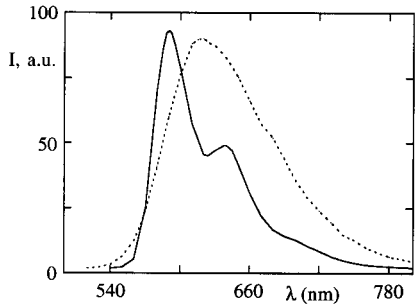

Figure 4. Luminescence spectra of **2** in MeOH/EtOH, 4:1 (v/v), at 77 K (solid line) and in acetonitrile solution at 298 K (dotted line). The spectra are uncorrected for photomultiplier response. Corrected values of emission maxima are reported in the main text.

with respect to **1** (>+2.00 V) is balanced by the more negative reduction potential of the acceptor ligand of the CT transition (i.e., L1 in **1** and $L1^-$ in **2**). The longer luminescence lifetime of **1** with respect to **2** at 77 K is probably due to different electron delocalization in the acceptor ligand of the MLCT excited state (as a consequence, a different distortion of the excited state with regard to the ground state can be inferred in the complexes, and such an effect translates into different coupling for nonradiative transitions[11]). Actually, the MLCT excited state in **1** involves the "symmetric" polyquinoline ligand L1 and in **2** it involves the "asymmetric" cyclometalating $L1^-$, and electron delocalization is expected to be more effective in the ligand L1. On passing to room temperature, the order of luminescence lifetimes is reversed (see above). This could suggest the involvement of an upper-lying excited state in the deactivation process of **1**. Work is in progress to investigate in detail the temperature dependence of the excited state properties of **1** and **2**.

Conclusion

Two novel bis-terdentate Ir(III)-cyclometalated compounds **1** and **2** have been prepared and characterized, and their absorption spectra, luminescence properties, and redox behavior have been studied. Because of their structures and of their spectroscopic, photophysical, and redox properties, **1** and **2** can be considered the first examples of a new class of luminescent and redox-active metal complexes. It can be envisaged that, after suitable functionalization of the ligands, these new chromophores could be inserted into metal-based supramolecular arrays for light energy conversion, thus opening a way to supramolecular architectures containing novel useful building blocks.

Experimental Section

Synthesis of 1 and 2. A mixture of the commercially available $IrCl_3$ (75 mg, 0.25 mmol) and bmpqpy[7b] (282 mg, 0.55 mmol) in glycerol (20 mL) was refluxed for 24 h under nitrogen. After cooling, 20 mL of water was added. The red-orange solution was further refluxed under stirring for 10 min and extracted with $CHCl_3$. The organic layer was rotary-evaporated to dryness, and CH_3CN was added. Repeated column chromatography on silica ($CH_3CN/KNO_3/H_2O$ (28:1:0.5) used as eluant) afforded two main fractions corresponding to complexes **1** ($R_f = 0.40$) and **2** ($R_f = 0.54$). Each fraction was rotary-evaporated to dryness, water (10 mL) was added, and the product was extracted with hot $CHCl_3$. The chloroform solution was dried on Na_2SO_4 and rotary-evaporated to dryness, and the crude product was dissolved in hot methanol (20 mL). A 20% aqueous solution of NH_4PF_6 (10 mL) was added. After the mixture was allowed to cool at room temperature, a red-orange powder precipitated, which was recovered by filtration, washed successively by cold water, methanol, and diethyl ether, and recrystallized from CH_2Cl_2/cyclohexane. This procedure gave 150 mg of **1** (40%) and 34 mg of **2** (10%). Both the new compounds gave satisfactory C, H, and N elemental analyses. Detailed NMR assignments and MS(FAB) data are as follows:[12]

1: orange-red solid. ^{1}H NMR (250 MHz; deuterated 1,1,2,2-tetrachloroethane, TCE): $\delta = 9.24$ (d, 1H(5) of $L1^-$, $J \approx 7.7$), 9.14 (d, 1H(3) of $L1^-$, $J \approx 7.7$), 8.89 (t, 1H(4) of $L1^-$, $J \approx 7.7$), 8.55 (m, 2H(3/5), of L1), 8.50 (bt, 1H(4) of L1), 8.42 (s, 1H(3′) *a* of $L1^-$), 8.14 (s, 2H(3′) of L1), 7.83 (m, 1H(5′) *a* of $L1^-$ + 1H(8′) *b* of $L1^-$ + 2H-(5′) of L1), 7.58 (m, 5H(Ph) *a* of $L1^-$ + 10H(Ph) of L1), 7.38 (m, 1H(6′) *a* of $L1^-$ + 2H(6′) of L1), 7.35 (bd, 1H(4″) *b* of $L1^-$), 7.10 (m, 2H(2″/6″) *b* of $L1^-$), 7.05 (bd, 1H(6′) *b* of $L1^-$), 6.55 (s, 2H(8′) of L1), 6.37 (d, 1H(5′) *b* of $L1^-$, $J \approx 8.5$), 6.25 (d, 2H(3″/5″) *b* of $L1^-$, $J \approx 7.3$), 5.85 (s, 1H(8′) *a* of $L1^-$), 2.42 (s, 3H(Me) *b* of $L1^-$), 2.18 (s, 6H(Me) of L1), 2.00 (s, 3H(Me) *a* of $L1^-$). MS(FAB^+): $m/z = 1218$; $[Ir(bmpqpy)(bmpqpy^-)]^{2+}$ requires 1218.

2: orange red solid. ^{1}H NMR (250 MHz; deuterated TCE): $\delta =$ 8.42 (d, 2H(5), $J \approx 7.3$), 8.16 (d, 2H(3), $J \approx 7.6$), 8.01 (t, 2H(4), $J \approx$ 7.9), 7.68 (d, 2H(5′) *a*, $J \approx 8.5$), 7.77 (s, 2H(8′) *b*), 7.53 (m, 10H(Ph) *a*), 7.23 (bd, 2H(6′) *a*), 7.21 (bd, 2H(4″) *b*), 7.03 (m, 2H(3″) *b* + 2H-(5″) *b*), 6.92 (dd, 2H(6′) *b*, $J \approx 8.8, 1.4$), 6.27 (bd, 2H(5′) *b* + 2H(6″) *b*), 6.18 (d, 2H(2″) *b*, $J \approx 7.6$), 6.11 (s, 2H(8′) *a*), 2.37 (s, 6H(Me) *b*), 1.95 (s, 6H(Me) *a*). MS(FAB^+): $m/z = 1217$; $[Ir(bmpqpy^-)_2]^+$ requires 1217.

Equipment and Procedures. Absorption spectra were obtained in acetonitrile solution at room temperature by means of a Kontron Uvikon 860 spectrophotometer. Luminescence spectra were obtained with a Perkin-Elmer LS-5B spectrofluorimeter. Emission lifetimes were measured with an Edinburgh FL-900 single-photon-counting instrument (nitrogen discharge; pulse width 3 ns). Emission quantum yields were measured at room temperature (20 °C) with the optically dilute method,[13] calibrating the spectrofluorimeter with a standard lamp. $[Ru(bpy)_3]^{2+}$ in aerated aqueous solution was used as a quantum yield standard, assuming a value of 0.028.[14] Electrochemical measurements were carried out in argon-purged acetonitrile solution at room temperature with a PAR 273 multipurpose instrument interfaced to a PC. The working electrode was a Pt microelectrode or a glassy carbon (8 mm^2, Amel) electrode. The counter electrode was a Pt wire, and the reference electrode was a SCE separated with a fine glass frit. The concentration of the complexes was 5×10^{-4} M, and tetraethylammonium hexafluorophosphate 0.05 M was used as supporting electrolyte. Cyclic voltammograms were obtained at sweep rates of 20, 50, 200, 500, and 1000 mV s^{-1}; DPV experiments were performed with a scan rate of 20 mV s^{-1}, a pulse height of 75 mV, and a duration of 40 ms. The same half-wave potential values are obtained from the DPV peaks and from the average of the cathodic and anodic cyclic voltammetric peaks. Both CV and DPV techniques have been used to measure the number of the exchanged electrons in each redox process,[15] utilizing 5×10^{-4} M ferrocene as reference compound. To establish the reversibility of a process, we used the criteria of (i) separation of 60 mV between cathodic and anodic peaks, (ii) close to unity ratio of the intensities of the cathodic and anodic currents, and (iii) constancy of the peak potential on changing sweep rate in the cyclic voltammograms. Experimental errors in the reported data are as follows: absorption maxima, 2 nm; emission maxima, 5 nm; emission lifetimes, 10%; emission quantum yields, 20%; redox potentials, 10 mV. As far as molar absorption coefficients are concerned, the uncertainly in their absolute values is ~10% because of the highly dilute solutions used (10^{-5}−10^{-4} M).

IC970791E

(11) Treadway, J. A.; Loeb, B.; Lopez, R.; Anderson, P. A.; Keene, F. R.; Meyer, T. J. *Inorg. Chem.* **1996**, *35*, 2242.

(12) For convenience, in NMR assignments the letter *a* labels resonances of the *a*-type phenyl and corresponding quinoline moieties, while the letter *b* labels *b*-type phenyl and corresponding quinoline moieties in $L1^-$ (see Figure 1). The assignments of the signals to each ligand are based on analysis of the H−H COSY 45 spectrum and on comparison with the data reported for complex **3**.[7b]

(13) Demas, J. N.; Crosby, G. A. *J. Phys. Chem.* **1971**, *75*, 991.

(14) Nakamaru, K. *Bull. Chem. Soc. Jpn.* **1982**, *55*, 2697.

(15) Campagna, S.; Denti, G.; Serroni, S.; Juris, A.; Venturi, M.; Ricevuto, V.; Balzani, V. *Chem. Eur. J.* **1995**, *1*, 211.